Proceedings of the 9ICEG
9th International Congress on Environmental Geotechnics
25-28 June, 2023 | Chania, Greece

https://doi.org/10.53243/ICEG2023-115

CO_2 storage in basalts: the impact of mineralisation on the hydromechanical response of the material

E. Stavropoulou[1], and L. Laloui[2]

[1]*Doctor, Ecole Polytechnique Fédérale de Lausanne (EPFL), Laboratory for Soil Mechanics (LMS), Lausanne, Switzerland, email: eleni.stavropoulou@epfl.ch*

[2]*Professor, Ecole Polytechnique Fédérale de Lausanne (EPFL), Laboratory for Soil Mechanics (LMS), Lausanne, Switzerland, email: lyesse.laloui@epfl.ch*

ABSTRACT

Carbon mineralisation in basalts is a promising cost-effective way to permanently store CO_2 in view of climate change mitigation. In this work, the impact of carbon mineralisation on the hydromechanical properties of a basaltic sample is studied. Unlike previous studies where CO_2 dissolved in fresh water is considered, here CO_2 dissolved in saline water is used aiming at a more ecological application of the technology at large scales. First, the flow properties of the material are measured in the lab before and after a 2-month exposure to dissolved CO_2 under field-representative conditions. Carbon mineralisation can substantially alter the pore space of the material, resulting in reduction of porosity, flow properties, and consequently overestimation of the injection and storage efficiency. The experimental results show a permeability reduction of half an order of magnitude, suggesting porosity reduction due to mineral precipitation. Image analysis of x-ray tomographies of the tested sample (resolution 50 µm/px) before and after CO_2 exposure show a total porosity reduction of 2.4 %. To better understand the evolution of the pore network before and after mineralisation, pore network simulations are performed on the real 3D porosity of the material acquired from the x-ray images. Two types of porosity are considered, macro (pores > 50 µm) and micro (solid matrix porosity). Reduction of the size of macro-pores does not impact flow. To reproduce the post-exposure flow results, decrease of the solid matrix porosity is required, revealing that carbon mineralisation is more prone to take place in the micro-pores.

Keywords: CO_2 storage, Basalts, carbon mineralisation, connected porosity, pore network model

1 INTRODUCTION

Carbon Capture and Storage (CCS) is receiving increasing attention worldwide as it is considered to be one of the most effective technologies towards climate change mitigation. Carbon mineralisation in basalts is a promising cost-effective technology for permanent CO_2 storage that has the great advantage of occurring very rapidly (1-2 years as per Matter et al, 2016; Clark et al., 2019) when compared to standard CCS solutions in sedimentary reservoirs (thousands of years). CO_2 is dissolved in water before injection in the subsurface, resulting in increased trapping safety, since solubility has already taken place. Injection is performed at low over-pressures at shallow depths of a few hundred metres in highly permeable locations. This results in reduced drilling operations and monitoring costs, as well as, in significantly lower risk of leakage to the surface (the injected fluid is not a buoyant fluid) or induced seismicity.

In terms of storage potential, abundant suitable basalt formations exist over the globe both off-shore or on-shore (Snæbjörnsdóttir et al, 2020). In Europe, CO_2 storage in basalts has been explored in Iceland (Carbfix) with a total injection for permanent mineralisation of more than 85'000 tons of CO_2 to date. Another field-scale project is ongoing in Hawaii (De Paolo et al., 2021) or previously conducted in the USA (Wallula project), where supercritical CO_2 was injected in a basaltic formation and up to 60% of mineralisation within two years has been estimated based on hydrological modelling (McGrail et al., 2017; White et al., 2020).

While storage of dissolved CO_2 in basalts has significant advantages as listed above, large-scale application would require substantial amounts of water that make this technology not ecologically viable. The use of seawater as a solute is an ideal alternative that is explored since recently in Iceland, where vast quantities are available in the immediate vicinity of the basaltic ocean crust, a reservoir with a storage potential of ~$3 \cdot 10^5$ Gt CO_2 (Marieni et al., 2013). Recent studies on basalt-seawater-CO_2 interaction showed that the efficiency of carbon mineralisation in seawater remains significant. Batch reactor testing revealed a total mineralisation of 20% of the initial injected CO_2 within five months, corresponding to carbonation rates similar to those observed in basalt-freshwater-CO_2 interaction experiments (lab and field) (Voigt et al., 2021).

In 2023, field injection of CO_2 dissolved in seawater will be performed for the first time by Carbfix at the Helguvík site. A highly fractured location is targeted for the injection at a depth below 400 m. Injection and therefore trapping efficiency relies on the flow properties of the basaltic material. Eventual porosity reduction (clogging) can significantly limit the storage potential of the material (Callow et al., 2018), which in the case of injection under constant flow rate, can lead to local increase of pore pressure, reduction of effective stress and triggering of micro-seismicity. While seismic exploration campaigns have never been conducted in the injection area, information on the extension of the reservoir and its properties are still limited.

The current work aims to provide a better insight into the efficiency of CO_2 mineralisation in the basaltic material and its impact on the material's hydromechanical properties with lab-scale testing and modelling. The transport properties of the material before and after exposure to dissolved CO_2 are targeted under pressure conditions representative of the field. Impact of eventual mineralisation on the pore space of the material is investigated with 3D with x-ray tomography. Finally, a pore network model (PNM) is employed to simulate fluid flow and understand the impact of carbon mineralisation on the connected porosity of the material.

2 TOOLS AND METHODOLOGY

2.1 Hydromechanical Testing of Basaltic Cores

Basalts are fine grained dark-coloured igneous rocks with 45 % to 85 % mafic minerals and are commonly located in extrusive volcanic settings (Farooqui et al., 2009). They are suitable formations for effective carbon mineralisation because of their high content in divalent cations (Ca^{2+}, Mg^{2+}, Fe^{2+}) and favourable mineral compositions (pyroxene and olivine) that are highly reactive to dissolved CO_2 (Snæbjörnsdóttir et al., 2020). In this study a basaltic core from a borehole located in the vicinity of the Helguvík site, where a distinct lava flow bedding has been identified. More precisely, the studied core originates from a shallow depth of ~20 m (BH-08) in the Hólmsberg cliff.

A cylindrical sample has been sized down from the basaltic core, to a diameter equal to 38 mm and a height of 78 mm. The flow properties of the basaltic sample are tested in the lab using the experimental setup illustrated in Figure 1. The sample is first confined at a pressure level of 5 MPa and saturated with synthetic saline water similar to the composition used by Voigt et al., 2021. The flow properties of the sample are then evaluated in terms of permeability and hydraulic conductivity. The measurement of permeability is performed with the constant head method (Darcy, 1856; Renard et al., 2001), applying a water pressure difference equal to 1 MPa between the upstream (2 MPa) and downstream (1 MPa) sides of the sample. The absolute permeability k (m^2) of the medium can be calculated through the hydraulic conductivity K (m/s), considering the fluid's density $\rho_f = 1.02$ g/cm^3, the acceleration of gravity g (m/s^2) and the fluid's dynamic viscosity $\eta_f = 1.05 \cdot 10^{-3}$ Pa·s:

$$k = K\frac{\eta_f}{\rho_f \cdot g} \qquad (1)$$

Based on the Darcy's law and neglecting the difference in elevation, the hydraulic conductivity can be calculated as follows:

$$K = Q_f \frac{\rho_f \cdot g \cdot L}{A \cdot \Delta P_f} \quad (2)$$

where, Q_f is the volumetric flow (m^3/s), L the height of the sample (m), A the area of the sample (m^2), ΔP_f (Pa) the applied pressure difference.

After the establishment of the initial flow properties of the sample, injection of CO_2 dissolved into saline water is performed. CO_2 is dissolved in the saline water in a reservoir at a pressure of 2 MPa and a volume of at least equal to the pore volume of the sample is injected. The two pore pressure valves (upstream and downstream) are then closed and the sample is left under no flow CO_2 exposure over a period of 2 months, at confining pressure 5 MPa and pore pressure 1.5 MPa, i.e. differential pressure equal to 3.5 MPa. A 2-month exposure time is chosen based on the observations reported by Voigt et al. 2021, where pH and mineral composition changes of seawater after 50 days interaction with basalt and CO_2. The flow properties of the sample are finally measured after CO_2 exposure by applying the same constant head method (ΔP = 1 MPa) and eventual carbon mineralisation is evaluated.

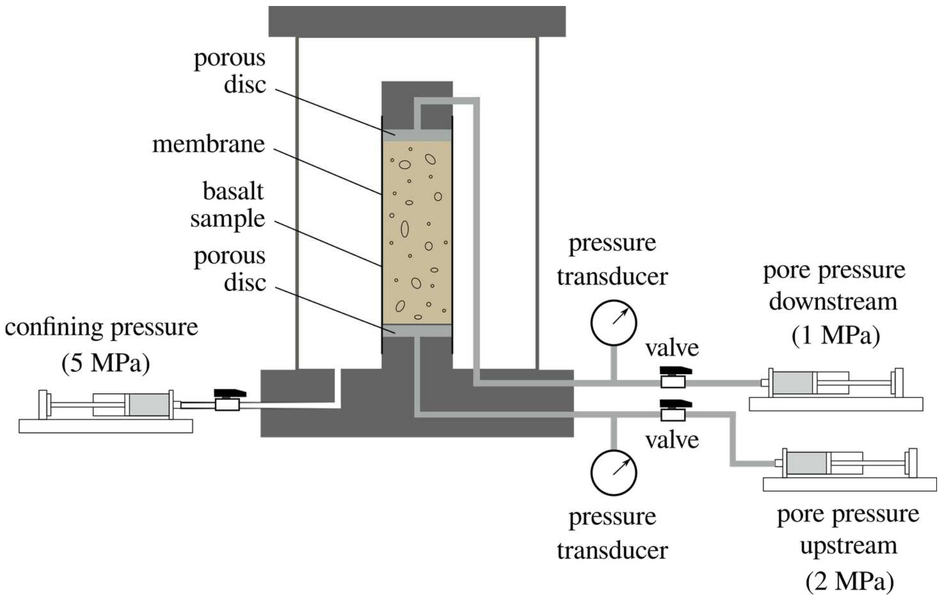

Figure 1. *Experimental setup for permeability measurement and CO_2 injection*

2.2 Pore Network Analysis

Carbon mineralisation is expected to alter the pore structure of the basaltic material. Mineral precipitation will result in reduction of the porosity and consequently reduction of the transport properties of the material. To understand the impact of mineralisation on the pore structure of the material, the tested sample has been scanned x-ray tomography (50 μm/px) before and after CO_2 exposure. Figure 2 shows a vertical and horizontal middle slice of 3D reconstructed x-ray image of the sample at its initial state, i.e. before CO_2 exposure. High heterogeneity of the pore space can be directly observed (black zones), with large pores at the bottom and denser zones at the top of the sample. Regardless the existence of very large pores (in the range of a few millimeters), flow is dominated by the connected porosity of the material, it is therefore of crucial importance to understand the connectivity of the tested sample.

To better understand the correlation between the pore structure of the material and the experimentally measured flow properties, a pore network model (PNM) is employed using the open source openPNM code (Gostick et. al, 2016). The 3D pore network is extracted directly from the x-ray image based on the SNOW algorithm (Gostick, 2017). More precisely, a binary image of the pores/solid matrix structure is used as input data. This algorithm uses a watershed segmentation method that defines the pore regions based on a calculated distance map from the solid matrix. The pore space is then described as a network of pores connected by throats that are represented by a spherical and cylindrical geometry respectively. To run the simulation a rectangular sample is required. For this purpose a maximal inscribed square region is extracted and considered, as shown in red frame in Figure 2.

Fluid flow simulation is performed using the Hagen-Poiseuille equation:

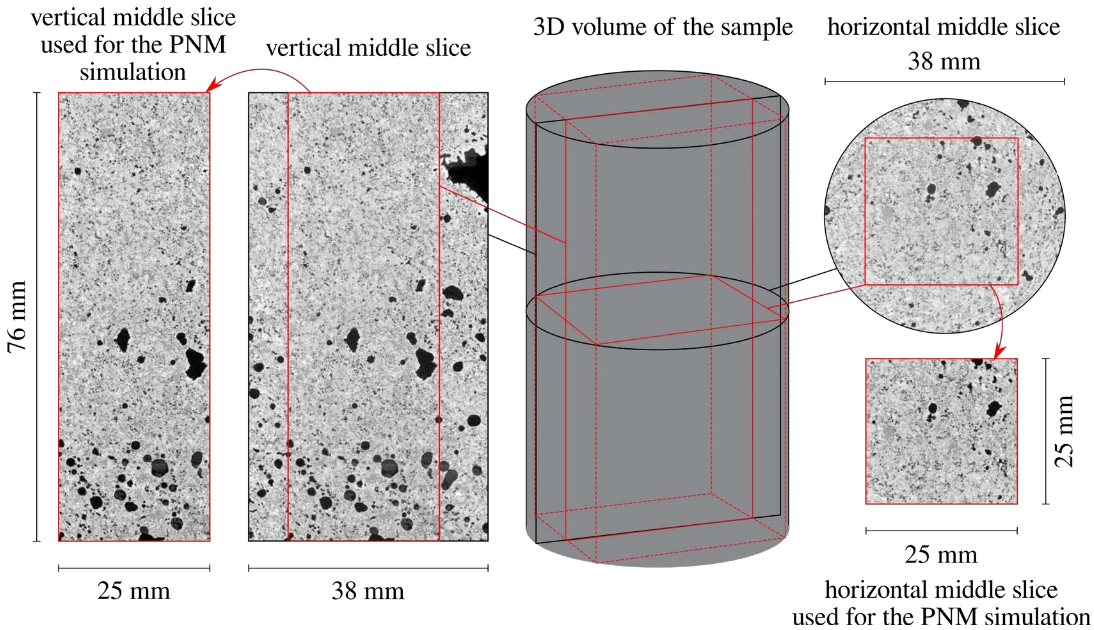

Figure 2. *Vertical and horizontal x-ray slices of the tested basaltic sample with pores represented by low greylevel zones (black zones); total volume tested in the lab (black frame), cropped volume for the simulation of the pore network model (PNM) (red frame).*

$$Q_{i,j} = \Delta P_{i,j} \frac{\pi \cdot r_{i,j}^4}{8 \cdot \mu_f \cdot L_{i,j}} \quad (3)$$

where $\Delta P_{i,j}$ (Pa) is the pressure difference between two consecutive pores *i, j*, $r_{i,j}$ (m) the radius of the throat connecting the two pores *i, j*, μ_f (Pa.s) the fluid's dynamic viscosity, $L_{i,j}$ (m) the distance between the two pores *i, j*, and $Q_{i,j}$ (m^3/s) the volumetric flow rate between the pores i, j.

The net flow rate Q of the sample is then obtained by summing up the flow rate of all pores, and the absolute permeability of the network is calculated based on the Darcy law (Equation 1). In this study, a single-phase laminar flow simulation is considered.

3 RESULTS

The experimental results of hydromechanical testing before and after CO_2 exposure are presented in Table 1. After two months of exposure to dissolved CO_2 in saline water, the flow properties of the basaltic sample have shown a reduction: the measured permeability has decreased by half an order of magnitude from $1.708 \cdot 10^{-16}$ m^2 to $7.572 \cdot 10^{-17}$ m^2. This result suggests that mineral precipitation has taken place over the exposure period, leading to reduction of the connected porosity and consequently flow. The obtained level of permeability is comparable to the experimental results reported by Callow et al., 2017 during flow testing with mineral water under a differential pressure of 4 MPa (~10^{-15} m^2). The higher permeability that they obtained can be explained by a sample of higher porosity (26.2 %), as well as the lower height/diameter ratio of the tested sample (0.6 instead of 2.0 in the current study).

Table 1. *Flow properties from hydromechanical testing before and after CO_2 exposure*

	Permeability, k (m^2)	**Hydraulic conductivity, K (m/s)**
Before CO_2 exposure	1.708E-16	1.650E-09
After CO_2 exposure	7.572E-17	7.318E-10

Reduced flow properties are supported by the porosity measurements from x-ray tomography. Based on the acquired x-ray images, an initial 3D porosity of 11.07 % is measured which decreases to 8.61 % after two months exposure to dissolved CO_2. However, it has not been possible to distinguish precise localised regions where pore size modification has taken place, at the given resolution. Thus, to gain a better insight in the evolution of the pore network from potential mineral precipitation, flow simulations are performed in the 3D pore network extracted from each x-ray image, i.e. before and after CO_2 exposure.

A pore network is assigned based on the input porosity image. In both images (pre- and post-CO_2 exposure), the pore architecture at the given resolution results in a poorly connected network in which flow throughout the entire height of the sample is not possible. In other words, at the given image resolution, a big number of visible pores (> 50 μm) is too far from their neighbour pores to be assigned connecting throats according to the watershed algorithm explained in detail by Gostick 2017. For this reason, the isolated pores, i.e. the non connected pores, are manually connected to the rest of the network by assigning a fixed throat diameter. This throat diameter is smaller than the minimum throat diameter of the initially generated pore network and represents the micro-porosity of the solid matrix of the material that cannot be detected from the scan resolution. In this way the connectivity of the material is represented by a double-scale porosity: macro-porosity (pores > 50 μm) and micro-porosity (solid matrix < 50 μm). The initial and final number of connecting throats of each pore network are reported in Table 2. A reduced number of connecting throats, i.e. connected pores, is calculated after CO_2 exposure, confirming a reduced connectivity in the network. The different steps for the creation of the fully connected network before initiating the flow simulation are presented in Figure 3.

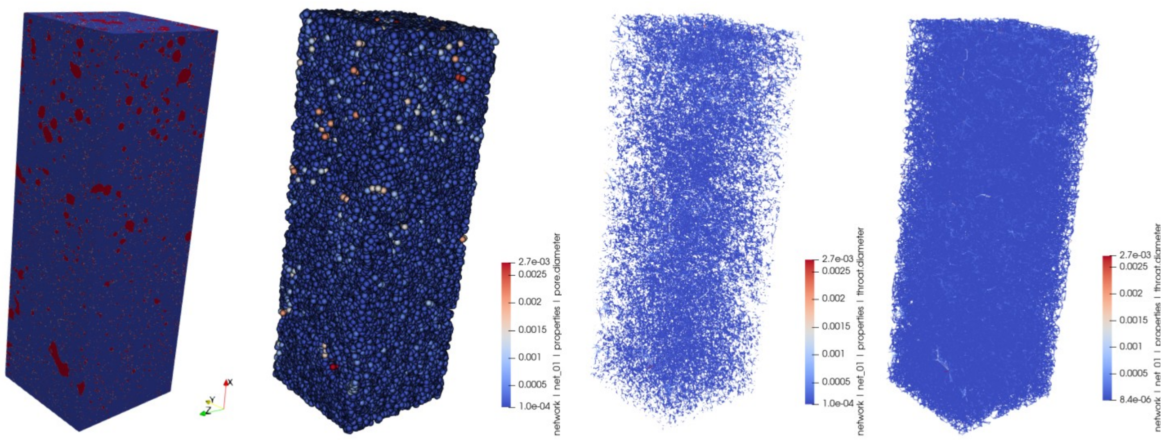

(a) (b) (c) (d)

Figure 3. *Initial pore structure before CO_2 exposure. (a) Binary input volume of pores (red) and solid (blue) from x-ray tomography, (b) Pore network created from the input x-ray image (color bar: pore diameter in m), (c) Initial connectivity (throats) of the pore network (color bar: throat diameter in m), (d) Fully connected network (color bar: throat diameter in m)*

Single-phase flow simulation is then performed under conditions similar to the hydromechanical tests in the lab. The resulting flow rates and permeability for both states of the sample are presented in Table 2 and are in good correspondence with the experimental values for a solid matrix throat diameter equal to 8.40 μm.

To confirm how the measured porosity reduction from the two x-ray images affects flow, the pore diameter of the fully connected pore network (pores > 50 μm) before CO_2 injection is decreased by the measured amount, i.e. by 2.4 %. Flow simulation of the modified network results only in a very slight reduction of permeability from $1.707 \cdot 10^{-16}$ m^2 to $1.694 \cdot 10^{-16}$ m^2. This response suggests that mineralisation in the macro-pores of the material does not impact flow in a significant way. Indeed, an additional reduction of micro-porosity, i.e. solid matrix porosity, is necessary to acquire the reduced post-exposure flow response, from 8.40 μm to 6.85 μm, confirming that flow is dominated by the narrower conduits as per Hagen Poisseuille flow definition. This result reveals that mineralisation is more prone to take place in the micro-pores, affecting the flow properties of the material by reduction of half an order of magnitude already after 2 months of exposure.

Table 2. *Pore network connectivity and resulting flow parameters from simulations based on the x-ray tomographies before and after CO_2 exposure*

	Initial number of pores/throats	**Final number of pores/throats**	**Permeability, k (m^2)**	**Flow rate, Q (m^3/s)**
Before CO_2 exposure	164815/85066	164815/356968	1.707E-16	3.895E-09
After CO_2 exposure	105208/43959	105208/211978	7.548E-17	1.722E-09

4 CONCLUSIONS

In this work, the impact of carbon mineralisation on the transport properties of a basaltic material have been investigated and demonstrated. The obtained experimental and modelling results provide an important insight into the occurrence of preferential mineralisation in the pore structure of the material by considering two distinct macro- and micro-porosity scales.

The following main findings can be summarised:

- Carbon mineralisation in the basaltic sample occurs already after a 2-month exposure of dissolved CO_2 in saline water. Mineralisation is confirmed by means of permeability reduction before and after CO_2 exposure in the lab (decrease by half an order of magnitude).
- Mineral precipitation is additionally indicated from 3D image analysis of x-ray tomographies of the tested sample before and after exposure. A reduction of total porosity by 2.4 % has been measured for an image resolution of 50 μm/px.
- To reproduce the flow properties of the tested sample from the pore network extracted from the sample's x-ray image, a double porosity must be assigned. In addition to the connected macro-pores, a micro-porosity representing the solid matrix pore size is set to 8.4 μm in order to reproduce a fully connected network.
- Reduction of the macro-pores by 2.4 % in the pore network simulation, i.e. porosity reduction from image analysis at the given resolution, does not have any significant impact on the acquired fluid flow. Reduction of the micro-porosity by 18.5 % is required to reproduce the post-CO_2 experimental results. This response suggests that carbon mineralisation is more prone to take place in the micro-pores of the material rather than the large pores.

The results of this study show that carbon mineralisation can impact the flow properties of the basaltic material, mainly by reduction of the micro-porosity. Successful implementation of the technology at large scales requires injection in locations of high porosity, ideally in fractured zones where flow can be ensured and mineralisation will not result in pore clogging.

5 ACKNOWLEDGEMENTS
This work is part of the DemoUpStorage project. The Authors would like to thank the Swiss Federal Office of Energy (SFOE) for the financial support.

REFERENCES

Abbott, A. B., Name2, C. D., Name3, E., & Name4, F. (2010). Settlement analysis of municipal solid waste. Journal of Environmental Engineering, 130(8), 1272-1279.

Callow, B., Falcon-Suarez, I., Ahmed, S., & Matter, J. (2018). Assessing the carbon sequestration potential of basalt using X-ray micro-CT and rock mechanics. *International Journal of Greenhouse Gas Control*, *70*, 146-156.

Clark, D. E., Galeczka, I. M., Dideriksen, K., Voigt, M. J., Wolff-Boenisch, D., & Gislason, S. R. (2019). Experimental observations of CO2-water-basaltic glass interaction in a large column reactor experiment at 50 C. International Journal of Greenhouse Gas Control, 89, 9-19.

Darcy, H.P.G. (1856). Les Fontaines publiques de la ville de Dijon. In: Exposition et application des principes à suivre et des formules à employer dans les questions de distribution d'eau, etc. V. Dalamont.

DePaolo, D. J., Thomas, D. M., Christensen, J. N., Zhang, S., Orr, F. M., Maher, K., Beson, S., Lautze, N., Xue, Z., & Mito, S. (2021). Opportunities for large-scale CO2 disposal in coastal marine volcanic basins based on the geology of northeast Hawaii. *International Journal of Greenhouse Gas Control*, *110*, 103396.

Farooqui, M. Y., Huijun Hou, Guoxin Li, Nigel Machin, Tom Neville, Aditi Pal, Chandramani Shrivastva et al. (2009). "Evaluating volcanic reservoirs." *Oilfield Review* 21, no. 1: 36-47.

Gostick J, Aghighi M, Hinebaugh J, Tranter T, Hoeh MA, Day H, Spellacy B, Sharqawy MH, Bazylak A, Burns A, Lehnert W. (2016). OpenPNM: a pore network modeling package. *Computing in Science & Engineering*. 25;18(4):60-74.

Gostick, J. T. (2017). Versatile and efficient pore network extraction method using marker-based watershed segmentation. *Physical Review E*, *96*(2), 023307.

Matter, J. M., Stute, M., Snæbjörnsdottir, S. Ó., Oelkers, E. H., Gislason, S. R., Aradottir, E. S., et al. (2016). Rapid carbon mineralization for permanent disposal of anthropogenic carbon dioxide emissions. Science, 352(6291), 1312-1314.

Marieni, C., Henstock, T. J., & Teagle, D. A. (2013). Geological storage of CO2 within the oceanic crust by gravitational trapping. *Geophysical Research Letters*, *40*(23), 6219-6224.

McGrail, B. P., Schaef, H. T., Spane, F. A., Horner, J. A., Owen, A. T., Cliff, J. B., ... & Sullivan, E. C. (2017). Wallula basalt pilot demonstration project: post-injection results and conclusions. *Energy Procedia*, *114*, 5783-5790.

Renard, P., Genty, A., Stauffer, F. (2001). Laboratory determination of the full permeability tensor. J. Geophys. Res.: Solid Earth 106 (B11), 26443–26452.

Snæbjörnsdóttir, S. Ó., Sigfússon, B., Marieni, C., Goldberg, D., Gislason, S. R., & Oelkers, E. H. (2020). Carbon dioxide storage through mineral carbonation. Nature Reviews Earth & Environment, 1(2), 90-102.

Voigt, M., Marieni, C., Baldermann, A., Galeczka, I. M., Wolff-Boenisch, D., Oelkers, E. H., & Gislason, S. R. (2021). An experimental study of basalt–seawater–CO2 interaction at 130° C. *Geochimica et Cosmochimica Acta*, *308*, 21-41.

White, S. K., Spane, F. A., Schaef, H. T., Miller, Q. R., White, M. D., Horner, J. A., & McGrail, B. P. (2020). Quantification of CO2 mineralization at the Wallula basalt pilot project. *Environmental Science & Technology*, *54*(22), 14609-14616.